



Research Article

Prostaglandin Production in Marine Diatom Heterologously Expressing Cyclooxygenase

Mayu Murakami¹, Miho Kikuchi¹, Yuto Kurizaki¹, Satoshi Murata¹, Yoshiaki Maeda², Hiroshi Tsugawa¹, Tsuyoshi Tanaka^{1*}

¹Division of Biotechnology and Life Science, Institute of Engineering, Tokyo University of Agriculture and Technology, 2-24-16 Naka-cho, Koganei, Tokyo, 183-8588, Japan

²Faculty of Life and Environmental Sciences, University of Tsukuba, 1-1-1 Tennoudai, Tsukuba, Ibaraki, 305-8572, Japan

*Corresponding author: tsuyo@cc.tuat.ac.jp; Tel.: +81423887401; Fax: +81423857713

Abstract: Prostaglandins (PGs) are biologically active molecules produced from C20 polyunsaturated fatty acids through the sequential actions of cyclooxygenase (COX) and various PG synthases. PGs are used for pharmaceutical purposes to induce labor and treat glaucoma. Currently, the market size of PGs was 17.5 billion US dollars in 2010. Commercial PGs are produced via chemical synthesis, which involves many reaction and purification steps, resulting in high production costs. In contrast, PG bioproduction using transgenic diatoms, which accumulate high amounts of C20 fatty acids (PG precursors), can be an eco-friendly alternative. However, PG production in microalgae remains limited. In this study, we examined the effect of newly identified diatom-derived cox genes on PG production in *Phaeodactylum tricornutum*, a model diatom that accumulates substantial amounts of eicosapentaenoic acid and arachidonic acid. Two cox genes from *Skeletonema marinoi* and *Thalassiosira rotula* were heterologously expressed, and PG production was detected only in the transformant expressing *T. rotula*-derived cox. The Trcox transformant exhibited a relative PG production level of 1.8, whereas the Smcox transformant produced no detectable PGs. The PG profile of the Trcox transformant consisted of 22.0% PGD₂, 30.0% PGE₂, 2.2% PGF_{2α}, 19.3% PGD₃, 19.7% PGE₃, and 6.9% PGF_{3α}. To the best of our knowledge, this is the first report to demonstrate the PGs production in transgenic *P. tricornutum* with the diatom-derived cox gene. These and the findings from our results may contribute to the further application of diatoms in the production of industrial PGs.

Keywords: Cyclooxygenase; Microalgae; Polyunsaturated fatty acid; Prostaglandins

1. Introduction

Prostaglandins (PGs) are a group of bioactive substances with a prostanoic acid skeleton (Miller, 2006). The diverse biological activities of PGs in mammals have been extensively investigated, such as blood pressure regulation (Swan and Breyer, 2011), smooth muscle contraction or relaxation (Xin et al., 2023; Ruan et al., 2011), and inflammatory response generation (Ricciotti and FitzGerald, 2011). PGs are used in a variety of pharmaceuticals due to their high bioactivity. For example, PGE₂ is utilized as a labor induction agent due to its cervical ripening and uterine contraction effects (Konopka et al., 2015). PGF_{2α} serves as both a labor induction agent and a glaucoma treatment, possessing uterine contraction effects similar to PGE₂. Additionally, PGF_{2α} promotes the excretion of intraocular aqueous humor, leading to a reduction in intraocular pressure (Coulthard et al., 2012). Furthermore, PGE₁ is an antiplatelet inhibitor owing to its ability to suppress platelet aggregation and dilate blood vessels (Marcolina et al., 2021). The market size for PGs was estimated to exceed US\$17.5 billion. Although PGs are primarily produced commercially through chemical synthesis, these methods require numerous reaction and purification processes (Peng and Chen, 2017; Coulthard et al., 2012). Therefore,

biological production of PGs has been suggested as an alternative approach.

PG is biologically synthesized from polyunsaturated fatty acids (PUFAs), such as arachidonic acid (20:4 [n-6], ARA) and eicosapentaenoic acid (20:5 [n-3], EPA), catalyzed by cyclooxygenase (COX). C20 PUFAs are converted to the unstable intermediate prostaglandin G (PGG) and then prostaglandin H (PGH). The introduction of heterologous *cox* genes has been shown to be a successful method for producing PGs in transgenic photosynthetic organisms, including *Arabidopsis thaliana* (Mohamed and Lazarus, 2014), the liverwort *Arabidopsis thaliana* (Takemura et al., 2013), and the diatom *Fistulifera solaris* (Maeda et al., 2021). In transgenic *A. thaliana*, mouse-derived *cox* genes were expressed along with enzymes involved in C20 PUFA biosynthesis, including $\Delta 9$ elongase, $\Delta 8$ desaturase, and $\Delta 5$ desaturase derived from microalgae and a fungus. After the confirmation of PGH generation in transgenic *A. thaliana*, protist-derived PGF (prostaglandin F) synthase (PGFS) was subsequently expressed, resulting in the production of approximately 8 ng/g of plant tissue of PGF_{2 α} (prostaglandin F_{2 α}) was produced. In the transgenic *M. polymorpha* derived from *Agarophyton vermiculophyllum* (AvCOX) expressing COX (Kanamoto et al., 2011), PGD₂ (prostaglandin D₂), PGE₂ (prostaglandin E₂) and PGF_{2 α} were produced, and the total PG content was 576 ng/g of dry weight. More recently, the introduction of the *Avcox* gene into the diatom *F. solaris*, which accumulates rich C20 fatty acids, resulted in the highest PGs production of 1290 ng/g of dry weight (e.g., PGD₂, PGE₂ and PGF_{2 α} derived from ARA and PGD₃, PGE₃ and PGF_{3 α} derived from EPA) (Maeda et al., 2021). Diatoms are a promising host for the biological production of PGs; however, the PG content remains infeasible for industrial use. Therefore, exploring new production hosts that can achieve higher productivity is essential.

Cox genes have recently been detected in the diatoms, *Thalassiosira rotula* (Di-Dato et al., 2020; Di-Dato et al., 2019) and *Skeletonema marinoi* (Di-Dato et al., 2017). Introduction of diatom-derived COX into desired hosts may improve PG production using diatoms; however, no reports of heterologous expression of diatom-derived COX exist, and its function is not yet understood. Microalgae are highly promising production hosts because of their rapid growth, high photosynthetic efficiency, and high lipid accumulation—often exceeding 50%–60% under certain conditions (Mirzayanti et al., 2024; Prihantini et al., 2021; Cercado et al., 2018). Moreover, their low environmental impact (Kartika et al., 2023) further highlights microalgae as sustainable and attractive bioproduction platforms. In this study, we aimed to evaluate PG production by heterologous expression of diatom-derived COX, which are *cox* genes from the diatom *S. marinoi* (*Smcox*) and *T. rotula* (*Trcox*), into a model diatom *Phaeodactylum tricornutum* as the PG production host. The whole genome analysis of *P. tricornutum* has been completed (Bowler et al., 2008), and a transgenic line has been established (Miyagawa et al., 2009). In addition, the lipids produced by *P. tricornutum* contain approximately 16% C20 fatty acids (EPA and ARA) (Yang et al., 2017), and it shows one of the highest C20 fatty acid productivity among model diatoms (Guo et al., 2024; Cui et al., 2019). Therefore, *P. tricornutum* has an ideal potential for the biological production of PGs. A significant amount of PGs production was confirmed in the *Trcox* transgenic *P. tricornutum*. On the other hand, the *Smcox*-expressing transformant showed no PG production. Our study, for the first time, showed the heterologous expression of diatom-derived *cox* genes to produce PGs using diatoms as a host. These findings may contribute to the further understanding of the function of COX in diatoms and their industrial use as PG production hosts.

2. Methods

2.1 Example Subsection

The marine diatom, *Phaeodactylum tricornutum*, was cultivated in a medium consisting of half the concentration of Guillard's f solution (f/2 medium) (Kang et al., 2011), which was dissolved in artificial seawater supplemented with 50 μ g/ml ampicillin to avoid bacterial contamination. For the cultivation of *P. tricornutum* transformant clones, the f/2 medium was modified

to include 100 $\mu\text{g}/\text{ml}$ zeocin (Thermo Fisher Scientific, Waltham, MA, USA). For qRT-PCR and PG production analyses, the cells were grown in flasks containing 600 mL of f/2 medium, with a starting cell concentration of 2.0×10^5 cells/mL. Cultivation was performed at 20°C under continuous light of 130 μmol photons/ m^2/s . Sterile air enriched with 2% CO_2 was bubbled through the culture at a flow rate of 0.8 l/l/min.

2.2 Prediction of the three-dimensional structure of diatom-derived cyclooxygenase

ColabFold (Kim et al., 2025) was used to predict the three-dimensional structure of COX derived from diatoms. The three-dimensional structure of *Ovis aries*-derived COX (PDB ID: 1DIY) was obtained from the Protein Data Bank. Pymol (Schrödinger, NY, USA) was used to visualize and align the 3D structure of the protein.

2.3 Plasmid construction and transformation

We used chemically synthesized DNA fragments encoding COX from *S. marinoi* and *T. rotula*. For expressing COX-GFP fusion proteins in *P. tricornutum*, two plasmids—pSP-SmCOX-GFP/shble and pSP-TrCOX-GFP/shble—were constructed based on the pSP-COX-GFP/GAPDH backbone. PCR-amplified *cox-gfp* fragments were assembled downstream of the *F. solaris* GAPDH promoter and upstream of the *P. tricornutum* fcpA terminator using the Gibson assembly. Similarly, the PCR-amplified *cox* gene fragment was inserted into the same regulatory context through Gibson assembly to generate a construct expressing COX without GFP.

Cells were bombarded with the Bio-Rad Biolistic PDS-1000/He particle delivery system (Bio-Rad Laboratories, CA, USA). Tungsten particles (median diameter 0.6 μm) were coated with 5 μg of plasmid DNA in the presence of 2.5 M CaCl_2 and 0.1 M spermidine. 5×10^7 cells were spread on f/2 medium agar and allowed to dry. The plates were placed in the second tier of the biolistic chamber, and bombardment was performed. After overnight recovery culture, the bombarded diatom cells were cultured on selection plates containing 100 $\mu\text{g}/\text{ml}$ zeocin. Colonies exhibiting zeocin resistance were inoculated into liquid f/2 medium containing 100 $\mu\text{g}/\text{mL}$ zeocin and cultured at 20°C under continuous illumination. The resulting clones were analyzed by PCR to verify the integration of the COX expression cassette into the genomic DNA.

2.4 Quantitative reverse transcription-PCR (qRT-PCR)

Total RNA was extracted from *P. tricornutum* cells (1×10^8 cells) using NucleoSpin RNA kit (MachereyNagel GmbH & Co. KG, Düren, Germany). cDNA was synthesized using the PrimeScrip RT reagent Kit with gDNA Eraser (Takara Bio Inc., Shiga, Japan) and purified using the QIAquick PCR Purification Kit (Qiagen k.k., Tokyo, Japan). The gene expression levels in the transformant clones were analyzed using the Applied Biosystems ViiA7 Real-time PCR System with Power SYBR® Green PCR Master Mix (Thermo Fisher Scientific, Waltham, MA, USA), the synthesized cDNA (2 ng), and primer sets targeting the *cox* or *rps* gene (Seibold et al., 2003). *Cox* expression levels were normalized to that of the *rps* gene.

2.5 Liquid chromatography mass spectrometry (LC-MS/MS)

PG extraction was conducted using a previously described method (Maeda et al., 2021) with some modifications. In brief, PGs (approximately 100 mg) were extracted from the lyophilized cells using ethyl acetate. High-performance liquid chromatography-tandem mass spectrometry (LC-MS/MS) was performed on the samples using a Nexera X2 UPLC (Shimadzu Co., Kyoto, Japan). An ACQUITY UPLC BEH C18 column (50 \times 2.1 mm: 1.7 μm) (Waters, U.S.A.) was used, and the column was maintained at 35°C and a flow rate of 300 $\mu\text{l}/\text{min}$. MS measurements were performed using LCMS-9030 (Shimadzu Co., Kyoto, Japan) in negative ion mode (DL temperature, 250°C; heat block temperature, 400°C; nebulizer gas, 3.0 l/min; drying gas, 10.0

l/min; collision energy, 20 ± 5 eV). The analysis targets were PGE₂-d₄ used as an internal standard, PG₂ derived from ARA (PGD₂, PGE₂, PGF_{2 α}), and PG₃ derived from EPA (PGD₃, PGE₃, PGF_{3 α}), which were determined to be 349.2020 m/z (PGD₃, PGE₃), 351.2176 m/z (PGD₂, PGE₂, PGF_{2 α}), and 353.2333 m/z (PGF_{3 α}).

3. Results and Discussion

3.1 Functional analysis based on prediction of the three-dimensional structure of diatom-derived cyclooxygenase

Recently, EPA-derived PG₃, ARA-derived PG₂, and DGLA-derived PG₁ have been detected in the diatoms *Thalassiosira rotula* (Di-Dato et al., 2020) and *Skeletonema marinoi* (Di-Dato et al., 2017). Transcriptome analysis of these two diatom species indicated COX; however, functional analysis was not conducted. Prior to gene introduction into *P. tricornutum*, we predicted the three-dimensional structures of *T. rotula*-derived COX (TrCOX) and *S. marinoi*-derived COX (SmCOX) using ColabFold (Mirdita et al., 2022) (Figure. 1(a) and Figure. 2(a)). Additionally, we compared the three-dimensional structures of the predicted models of diatom-derived COX with *Ovis aries*-derived COX structure, which was already determined by X-ray crystallographic structure analysis. (Figure. 1(b) and Figure. 2(b)). The amino acid sequence similarity of TrCOX and SmCOX to *O. aries*-derived COX was 27.55% and 29.46%, respectively, yet the overall folds were well conserved. The root mean square deviation (RMSD) (Vlachakis et al., 2013) of atomic positions, an indicator of protein structural similarity, is shown in Figure 3 to support the structural similarity. As a result, most of the predicted three-dimensional structures of diatom-derived COX showed higher similarity with those of *O. aries*-derived COX. In mammalian COX-1, Tyr385 forms a tyrosyl radical and initiates the COX reaction by removing the pro-S hydrogen from the 13th position of arachidonic acid. Also, His388 is known as the proximal heme ligand (Seibold et al., 2003). These amino acid residues are essential for enzyme activity and are conserved in the PGH synthase family (Varvas et al., 2013). These amino acid residues were conserved in TrCOX and SmCOX, similar to mammalian COXs. In addition, Trp387 and Tyr348, which are involved in PGG production via the cyclization reaction and function in properly positioning the C13 position in ARA, are retained in diatom-derived COX (Figure 4).

Although these residues are conserved and are typically associated with catalytic capability, functional assays revealed clear differences between TrCOX and SmCOX. PG production was observed only in *P. tricornutum* expressing TrCOX, while SmCOX showed no detectable activity. Accordingly, subtle structural differences, such as the conformation of the substrate-binding pocket, the orientation of essential residues, or cofactor accessibility, may critically affect enzyme activity, despite the presence of conserved catalytic residues that function as PG endoperoxide synthases (Seo and Oh, 2017). Furthermore, both diatom-derived COXs were conserved in Tyr385 and His388, which are essential for radical formation and heme binding (Seibold et al., 2003). Likewise, residues such as Trp387 and Tyr348, which are involved in substrate cyclization and positioning, were also retained (Varvas et al., 2013). Nevertheless, mutagenesis studies have shown that even minor alterations near these catalytic residues or within the substrate-binding channel, including mutations at Val349, Ile523, and Leu384, can abolish or markedly reduce enzymatic activity (Varvas et al., 2013). In addition, recent structural analyses of COX-inhibitor complexes demonstrated that subtle conformational shifts in the substrate access channel can significantly alter catalytic efficiency and ligand binding (Rouzer and Marnett, 2020). According to these insights, small conformational differences in the substrate-binding pocket or cofactor access pathway may explain the lack of SmCOX activity under our experimental conditions. The numbering of the residues used here corresponds to the amino acids on ovine COX.

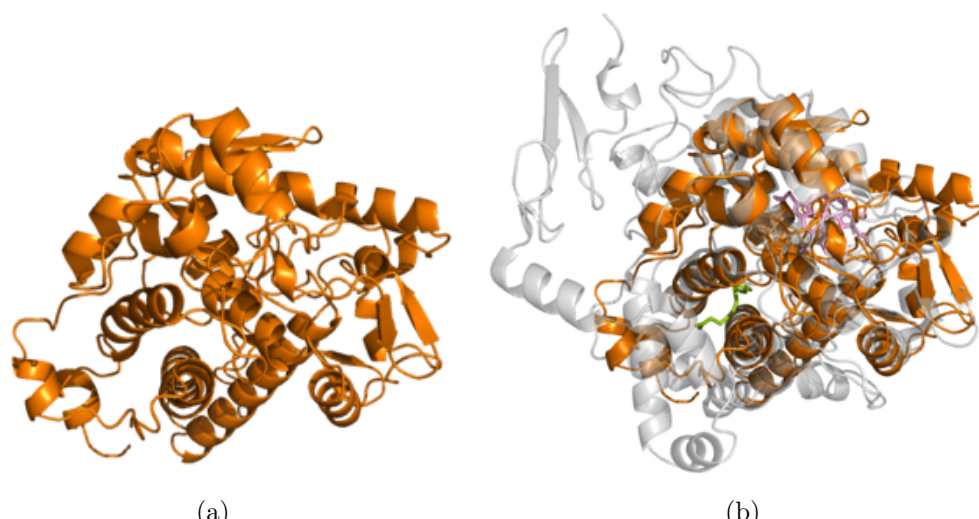


Figure 1 Comparison of the modeled TrCOX structure (orange) and the sheep COX X-ray structure (gray). (a) Superposition of the modeled TrCOX structure (orange) and (b) overlay of the two COX Structures

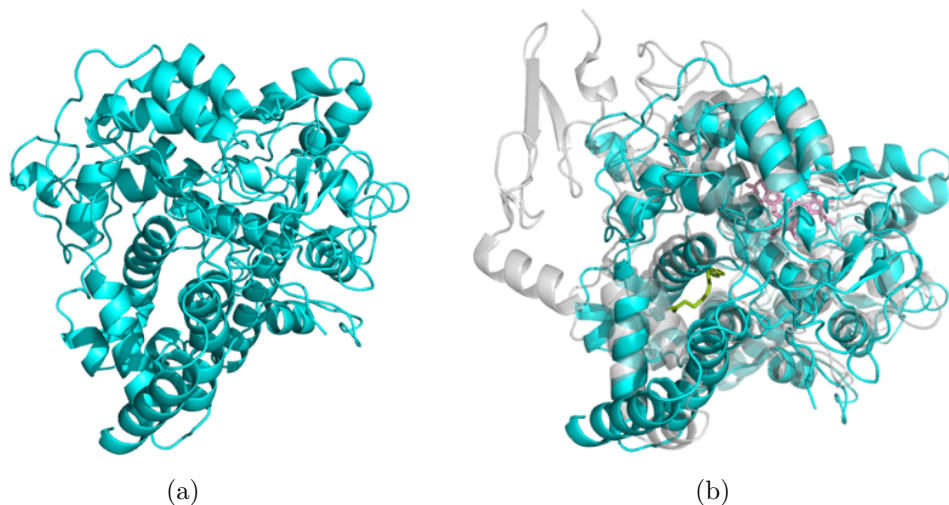


Figure 2 Comparison of the modeled SmCOX structure (blue) and the sheep COX X-ray structure (gray). (a) Superposition of the modeled SmCOX structure (blue) and (b) Overlay of the two COX structures

3.2 Development of diatom-derived transformants expressing COX

We generated transformants expressing diatom-derived COX to experimentally verify enzyme activity. The pSP-SmCOX-GFP/shble vector was introduced into *P. tricornutum* by particle bombardment, and 342 zeocin-resistant colonies were subjected to PCR amplification to detect the presence of the target gene. The presence of the Smcox gene was confirmed in 61 clones among the obtained colonies. After RT-qPCR gene expression analysis, cox gene expression was confirmed in the clone named Smcox_1, and this clone was selected for further analysis (Figure 5(a)). The pSP-TrCOX-GFP/shble vector was also introduced into *P. tricornutum*, and PCR amplification was conducted on 88 zeocin-resistant colonies. Among the 5 clones which showed the presence of Trcox genes, Trcox_1 showed a relatively high expression level and was used for further analysis (Figure 5(b)). As the cox genes in transformants were fused with *gfp* genes, fluorescence microscopic analysis was conducted for both Smcox_1 and Trcox_1 to evaluate COX localization. GFP fluorescence was confirmed in the Smcox_1 strain (Figure 6). GFP fluorescence in the Smcox_1 strain was observed in the cytoplasm. Fluorescent microscopy confirmed cytoplasmic localization in the Trcox_1 strain, which is consistent with the ability of COX to access free fatty acids.

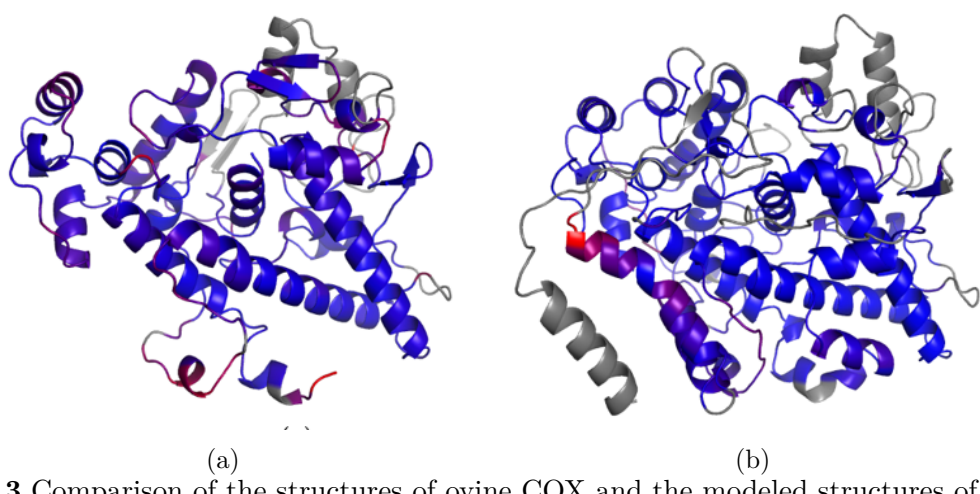


Figure 3 Comparison of the structures of ovine COX and the modeled structures of diatom COXs. The blue, red, and gray regions represent structures with high, low, and no similarities, respectively. Respectively, between the two compared COXs. Comparison in TrCOX (a) and SmCOX (b)

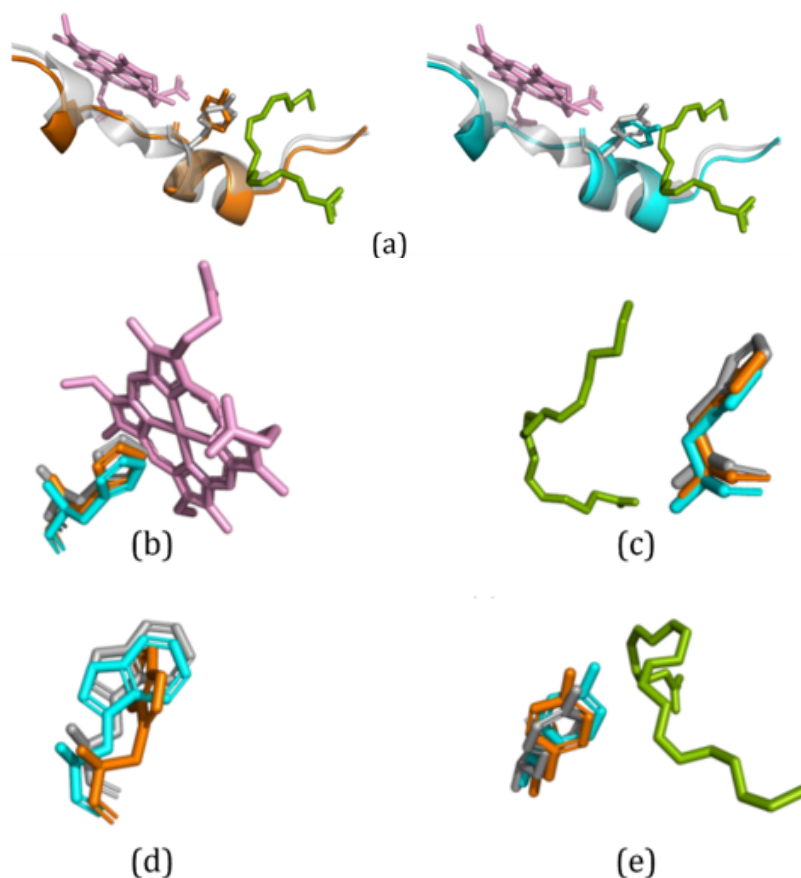


Figure 4 Comparison of important amino acid residues derived from diatoms and mammals for COX to function. The predicted TrCOX structure is shown in orange. The predicted SmCOX structure in cyan. Ovine COX (PDB ID: 1DIY) is shown in gray. Heme is in pink.

The substrate is in light green. (a) Heme binding site and Tyr385 is important for cyclooxygenase activity. (b) His388 is the proximal heme ligand. (c) Histidin in the substrate-binding site. (d) Trp387 is important for PG formation through cyclization. (e) Tyr348 is essential for the proper positioning of C-13 in ARA

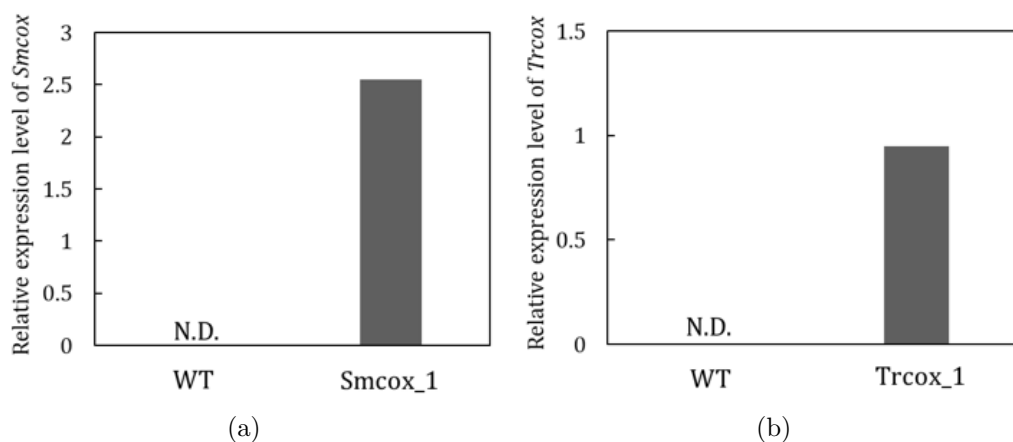


Figure 5 Real-time polymerase chain reaction analysis of *P. tricornutum* wild type (WT) and transformants. The expression cox gene levels were normalized using the *rps* gene as a reference gene for internal control

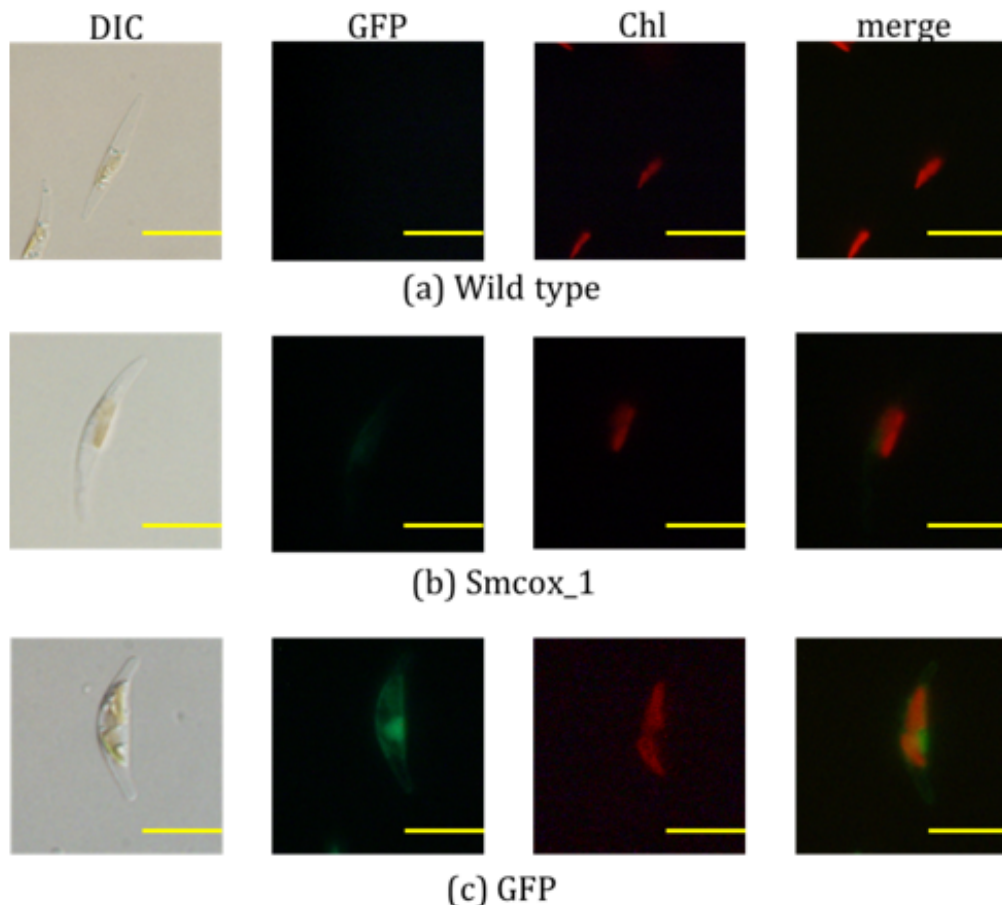


Figure 6 Localization analysis of GFP fused with SmCOX in *P. tricornutum*. Chloroplasts and GFP are shown in red and green, respectively. (a) Wild type (b) SmCOX-GFP is located in the cytosol. (c) The transformant expressing only GFP, fluorescence is located in the cytosol (scale bar = 5 μ m)

3.3 Evaluation of PG production in diatom-derived COX-expressing transformants

In this study, the relative production of PGs was determined using LC-MS/MS. PG production was not detected in the Smcox_1 strain (i.e., the peak intensity was lower than the background level). On the other hand, in the Trcox_1 strain, PG production was observed,

with a relative production level of 1.8 (Figure 7). TrCOX catalyzes the conversion of ARA and EPA into PGH₂ and PGH₃. Subsequently, the unstable PGH was converted into prostaglandin D (PGD), prostaglandin E (PGE), and prostaglandin F (PGF) non-enzymatically at a ratio of 1:3:0.1 (Yu et al., 2011; Siaut et al., 2007). In the Trcox1 strain, the composition of the produced PG was as follows: 19.3% PGD₃, 19.7% PGE₃, 6.9% PGF_{3α}, 22.0% PGD₂, 30.0% PGE₂, and 2.2% PGF_{2α}.

This observed PG production in Trcox_1 highlights that *P. tricornutum* provides sufficient free C20 fatty acids as precursors, unlike *F. solaris*, where fatty acids are largely stored in oil bodies. This difference in host lipid metabolism likely influences PG productivity. In fact, in previous studies using the oleaginous diatom *F. solaris*, the PG content in dry biomass remained too low for practical application. *F. solaris* has a large intracellular oil body, indicating that most C20 fatty acids are sequestered in oil bodies and that free fatty acids in the cytoplasm are limited. Therefore, one limiting factor in PG production using *F. solaris* is the accessibility of COX to C20 fatty acids, since the introduced enzyme localizes in the cytoplasm (Varvas et al., 2013). In contrast, in *P. tricornutum*, free C20 fatty acids, such as PG precursors, are more abundant in the cytoplasm than those sequestered in oil bodies, such as triacylglycerols.

This study provides the first report on PG production in diatoms through heterologous expression of diatom-derived COX. Although PG production using diatom-derived COX has been demonstrated, knowledge about its function remains limited. Further analyses are necessary to deepen our understanding of diatom-derived COX function and to improve PG productivity. Moreover, the findings indicate that *P. tricornutum* is a more suitable host than *F. solaris* for PG production due to differences in lipid metabolism and precursor availability. Continued structural, functional, and metabolic engineering efforts are expected to further enhance PG productivity in diatoms.

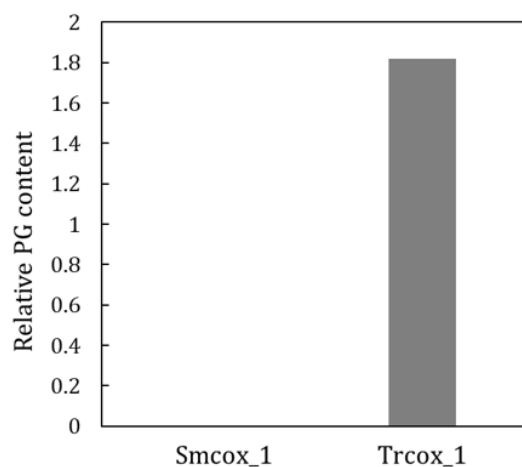


Figure 7 Total PG production of Smcox_1 and Trcox_1 transformants

4. Conclusions

In this study, we evaluated PG production in the genetically modified diatom *P. tricornutum* expressing diatom-derived COX. Functional analysis based on the predicted three-dimensional structure of diatom-derived cyclooxygenase showed that both TrCOX and SmCOX have conserved functional domains and function as PG endoperoxide synthases. For the first time, PG production using diatom-derived cox genes was demonstrated in Trcox_1. Our findings emphasized the potential of diatom-derived COX for the future practical use of biological PG production using *P. tricornutum* as a host.

Acknowledgements

This study was supported by JSPS KAKENHI Grant-in-Aid for Scientific Research A [grant number 24H00392] (granted to T. T.) and by JST Grant Number JPMJPF2104.

Author Contributions

Mayu Murakami contributed to data analyses, writing the original manuscript, and editing. Miho Kikuchi, Yuto Kurizaki and Hiroshi Tsugawa contributed to acquisition and analyses of data, and editing. Satoshi Murata and Yoshiaki Maeda performed data analyses and editing. Tsuyoshi Tanaka designed conceptualization, data analyses, and editing. All authors discussed the data and proof-read the manuscript.

Conflict of Interest

The authors declare that there are no conflicts of interests.

Declaration of AI

The authors declare that no artificial intelligence tools were used in the writing, data analysis, or figure preparation of this manuscript.

References

Bowler, C., Allen, A. E., Badger, J. H., Grimwood, J., Jabbari, K., Kuo, A., & Grigoriev, I. V. (2008). The *phaeodactylum* genome reveals the evolutionary history of diatom genomes. *Nature*, 456(7219), 239–244. <https://doi.org/https://doi.org/10.1038/nature07410>

Cercado, A. P., Ballesteros, F. C., & Capareda, S. C. (2018). Biodiesel from three microalgae transesterification processes using different homogeneous catalysts. *International Journal of Technology*, 9(4), 645–651. <https://doi.org/https://doi.org/10.14716/ijtech.v9i4.1145>

Coulthard, G., Erb, W., & Aggarwal, V. K. (2012). Stereo-controlled organocatalytic synthesis of prostaglandin pgf in seven steps. *Nature*, 489(7415), 278–281. <https://doi.org/https://doi.org/10.1038/nature11411>

Cui, Y., Thomas-Hall, S. R., & Schenk, P. M. (2019). Phaeodactylum tricornutum microalgae as a rich source of omega-3 oil. *Food Chemistry*, 297, 124937. <https://doi.org/https://doi.org/10.1016/j.foodchem.2019.06.004>

Di-Dato, V., Barbarinaldi, R., Amato, A., Di Costanzo, F., Fontanarosa, C., Perna, A., Amoresano, A., Esposito, F., Cutignano, A., Ianora, A., & Romano, G. (2020). Variation in prostaglandin metabolism during growth of the diatom *thalassiosira rotula*. *Scientific Reports*, 10, 5374. <https://doi.org/https://doi.org/10.1038/s41598-020-61967-3>

Di-Dato, V., Di Costanzo, F., Barbarinaldi, R., Perna, A., Ianora, A., & Romano, G. (2019). Unveiling the presence of biosynthetic pathways for bioactive compounds in the *thalassiosira rotula* transcriptome. *Scientific Reports*, 9, 9893. <https://doi.org/https://doi.org/10.1038/s41598-019-46276-8>

Di-Dato, V., Orefice, I., Amato, A., Fontanarosa, C., Amoresano, A., Cutignano, A., Ianora, A., & Romano, G. (2017). Animal-like prostaglandins in marine microalgae. *The ISME Journal*, 11(7), 1722–1726. <https://doi.org/https://doi.org/10.1038/ismej.2017.27>

Guo, W., Weng, Y., Ma, W., Chang, C., Gao, Y., Huang, X., & Zhang, F. (2024). Improving lipid content in the diatom *phaeodactylum tricornutum* by the knockdown of the enoyl-coa hydratase using crispr interference. *Current Issues in Molecular Biology*, 46(10), 10923–10933. <https://doi.org/https://doi.org/10.3390/cimb46100649>

Kanamoto, H., Takemura, M., & Ohyama, K. (2011). Identification of a cyclooxygenase gene from the red alga *gracilaria vermiculophylla* and bioconversion of arachidonic acid to pgf in engineered *escherichia coli*. *Applied Microbiology and Biotechnology*, 91(4), 1121–1129. <https://doi.org/https://doi.org/10.1007/s00253-011-3349-5>

Kang, K. H., Qian, Z. J., Ryu, B., & Kim, S. K. (2011). Characterization of growth and protein contents from microalgae navicula incerta with the investigation of antioxidant activity of enzymatic hydrolysates. *Food Science and Biotechnology*, 20(1), 183–191. <https://doi.org/https://doi.org/10.1007/s10068-011-0025-6>

Kartika, R., Ritonga, A. H., Sulastri, L., Nurliana, S., Irawan, D., & Simanjuntak, P. (2023). Biosorption of hexavalent chromium Cr(VI) using microalgae *Scenedesmus* sp as environmental bioindicator. *International Journal of Technology*, 14(4), 791–799. <https://doi.org/https://doi.org/10.14716/ijtech.v14i4.5188>

Kim, G., Lee, S., Karin, E. L., Kim, H., Moriwaki, Y., Ovchinnikov, S., Steinegger, M., & Mirdita, M. (2025). Easy and accurate protein structure prediction using ColabFold. *Nature Protocols*, 20(3), 620–642. <https://doi.org/https://doi.org/10.1038/s41596-024-01060-5>

Konopka, C. K., Glanzner, W. G., Rigo, M. L., Rovani, M. T., Comim, F. V., Gonçalves, P. B. D., Morais, E. N., Antoniazzi, A. Q., Mello, C. F., & Cruz, I. B. M. (2015). Responsivity to PGE2 labor induction involves concomitant differential prostaglandin E receptor gene expression in cervix and myometrium. *Genetics and Molecular Research*, 14(3), 10877–10887. <https://doi.org/https://doi.org/10.4238/2015.September.9.25>

Maeda, Y., Tsuru, Y., Matsumoto, N., Nonoyama, T., Yoshino, T., Matsumoto, M., & Tanaka, T. (2021). Prostaglandin production by the microalga with heterologous expression of cyclooxygenase. *Biotechnology and Bioengineering*, 118(7), 2734–2743. <https://doi.org/https://doi.org/10.1002/bit.27792>

Marcolina, A., Vu, K., & Annaswamy, T. M. (2021). Lumbar spinal stenosis and potential management with prostaglandin E1 analogs. *American Journal of Physical Medicine and Rehabilitation*, 100(3), 297–302. <https://doi.org/10.1097/PHM.0000000000001620>

Miller, S. B. (2006). Prostaglandins in health and disease: An overview. *Seminars in Arthritis and Rheumatism*, 36(1), 37–49. <https://doi.org/https://doi.org/10.1016/j.semarthrit.2006.03.005>

Mirdita, M., Schütze, K., Moriwaki, Y., Heo, L., Ovchinnikov, S., & Steinegger, M. (2022). ColabFold: Making protein folding accessible to all. *Nature Methods*, 19(6), 679–682. <https://doi.org/https://doi.org/10.1038/s41592-022-01488-1>

Mirzayanti, Y. W., Marlinda, L., Irawan, H., Al Muttaqii, M., Ma'sum, Z., Asri, N. P., & Chern, J. M. (2024). Performance of in-situ stirring batch reactor transesterification of *nannochloropsis* sp microalgae into biodiesel. *International Journal of Technology*, 15(4), 859–869. <https://doi.org/https://doi.org/10.14716/ijtech.v15i4.6678>

Miyagawa, A., Okami, T., Kira, N., Yamaguchi, H., Ohnishi, K., & Adachi, M. (2009). High efficiency transformation of the diatom *Phaeodactylum tricornutum* with a promoter from the diatom *Cylindrotheca fusiformis*. *Phycological Research*, 57(2), 142–146. <https://doi.org/https://doi.org/10.1111/j.1440-1835.2009.00531.x>

Mohamed, M. E., & Lazarus, C. M. (2014). Production of prostaglandins in transgenic *Arabidopsis thaliana*. *Phytochemistry*, 102, 74–79. <https://doi.org/https://doi.org/10.1016/j.phytochem.2014.02.013>

Peng, H., & Chen, F. E. (2017). Recent advances in asymmetric total synthesis of prostaglandins. *Organic and Biomolecular Chemistry*, 15(30), 6281–6301. <https://doi.org/10.1039/C7OB01341H>

Prihantini, N. B., Maulana, F., Wardhana, W., Takarina, N. D., Nurdin, E., Handayani, S., Nasruddin, & Haryani, G. S. (2021). Wild mixed culture microalgae biomass from Lake Agathis harvested directly using ultrasound harvesting module as biofuel raw material. *International Journal of Technology*, 12(5), 1081–1090. <https://doi.org/https://doi.org/10.14716/ijtech.v12i5.5226>

Ricciotti, E., & Fitzgerald, G. A. (2011). Prostaglandins and inflammation. *Arteriosclerosis, Thrombosis, and Vascular Biology*, 31(5), 986–1000. <https://doi.org/https://doi.org/10.1161/ATVBAHA.110.207449>

Rouzer, C. A., & Marnett, L. J. (2020). Structural and chemical biology of the interaction of cyclooxygenase with substrates and non-steroidal anti-inflammatory drugs. *Chemical Reviews*, 120(15), 7592–7641. <https://doi.org/https://doi.org/10.1021/acs.chemrev.0c00215>

Ruan, Y. C., Zhou, W., & Chan, H. C. (2011). Regulation of smooth muscle contraction by the epithelium: Role of prostaglandins. *Physiology*, 26(3), 156–170. <https://doi.org/10.1152/physiol.00036.2010>

Seibold, S. A., Ball, T., Hsi, L. C., Mills, D. A., Abeysinghe, R. D., Micielli, R., Rieke, C. J., Culier, R. I., & Smith, W. L. (2003). Histidine 386 and its role in cyclooxygenase and peroxidase catalysis by prostaglandin-endoperoxide h synthases. *Journal of Biological Chemistry*, 278(46), 46163–46170. <https://doi.org/https://doi.org/10.1074/jbc.M306319200>

Seo, M. J., & Oh, D. K. (2017). Prostaglandin synthases: Molecular characterization and involvement in prostaglandin biosynthesis. *Progress in Lipid Research*, 66, 50–68. <https://doi.org/https://doi.org/10.1016/j.plipres.2017.04.003>

Siaut, M., Heijde, M., Mangogna, M., Montsant, A., Coesel, S., Allen, A., Manfredonia, A., Falciatore, A., & Bowler, C. (2007). Molecular toolbox for studying diatom biology in *phaeodactylum tricornutum*. *Gene*, 406(1–2), 23–35. <https://doi.org/https://doi.org/10.1016/j.gene.2007.05.022>

Swan, C. E., & Breyer, R. M. (2011). Prostaglandin e2 modulation of blood pressure homeostasis: Studies in rodent models. *Prostaglandins, Other Lipid Mediators*, 96(1–4), 10–13. <https://doi.org/https://doi.org/10.1016/j.prostaglandins.2011.07.001>

Takemura, M., Kanamoto, H., Nagaya, S., & Ohyama, K. (2013). Bioproduction of prostaglandins in a transgenic liverwort, *marCHANTIA polymorpha*. *Transgenic Research*, 22(5), 905–911. <https://doi.org/https://doi.org/10.1007/s11248-013-9699-2>

Varvas, K., Kasvandik, S., Hansen, K., Järving, I., Morell, I., & Samel, N. (2013). Structural and catalytic insights into the algal prostaglandin h synthase reveal atypical features of the first non-animal cyclooxygenase. *Biochimica et Biophysica Acta*, 1831(4), 863–871. <https://doi.org/https://doi.org/10.1016/j.bbapap.2012.11.010>

Vlachakis, D., Pavlopoulou, A., Kazazi, D., & Kossida, S. (2013). Unraveling microalgal molecular interactions using evolutionary and structural bioinformatics. *Gene*, 528(2), 109–119. <https://doi.org/https://doi.org/10.1016/j.gene.2013.07.039>

Xin, Q., Yu, G., Feng, I., & Dean, J. (2023). Chromatin remodeling of prostaglandin signaling in smooth muscle enables mouse embryo passage through the female reproductive tract. *Developmental Cell*, 58(18), 1716–1732.e8. <https://doi.org/https://doi.org/10.1016/j.devcel.2023.08.025>

Yang, Y. H., Du, L., Hosokawa, M., Miyashita, K., Kokubun, Y., Arai, H., & Taroda, H. (2017). Fatty acid and lipid class composition of the microalga *phaeodactylum tricornutum*. *Journal of Oleo Science*, 66(4), 363–368. <https://doi.org/https://doi.org/10.5650/jos.ess16205>

Yu, R., Xiao, L., Zhao, G., Christman, J. W., & van Breemen, R. B. (2011). Competitive enzymatic interactions determine the relative amounts of prostaglandins e2 and d2. *The Journal of Pharmacology and Experimental Therapeutics*, 339(2), 716–725. <https://doi.org/https://doi.org/10.1124/jpet.111.185405>